

V.L. KALASHNIKOV¹
P. DOMBI¹
T. FUJI¹
W.J. WADSWORTH²
J.C. KNIGHT²
P.S.J. RUSSELL²
R.S. WINDELER³
A. APOLONSKI^{1,4} ✉

Maximization of supercontinua in photonic crystal fibers by using double pulses and polarization effects

¹ Institut für Photonik, Technische Universität Wien, Gusshausstrasse 27/387, 1040 Wien, Austria
² Optoelectronics Group, Department of Physics, University of Bath, Bath BA2 7AY, UK
³ OFS Laboratories, 700 Mountain Avenue, Murray Hill, NJ 07974, USA
⁴ Institute of Automation and Electrometry, SB RAS, Novosibirsk 630090, Russia

Received: 4 February 2003 / Revised version: 22 April 2003
Published online: 24 June 2003 • © Springer-Verlag 2003

ABSTRACT We show with sub-20 fs pulses both experimentally and theoretically two techniques to control the width and polarization of spectral supercontinua generated in photonic crystal fibers. The first exploits double pulses which interact inside the fiber nonelastically due to stimulated Raman scattering and thus make the supercontinuum wider, whereas the peak intensity can be kept at a reasonably moderate level to prevent fiber damage. The second approach includes polarization manipulations which allow a desirable polarization state to be obtained in a definite spectral range and the spectral shape and width to be varied.

PACS 42.65.Tg; 42.81.Dp

1 Introduction

Generation of spectral supercontinuum (SC) is a well-known effect [1] which became a hot topic in optics in recent years to a certain extent due to photonic crystal fibers (PCFs) [2, 3]. The SC is a key prerequisite for the generation of short pulses [4, 5] and it can also be considered as a broadband comb of equidistant frequencies for high-resolution spectroscopy [6]. There exist some limitations in experiments where the SC is generated: (i) in almost every case it is better to keep the fiber length as short as possible to increase the transmittance through it and to decrease the spectral noise [7]; (ii) the input pulse power (energy) has to be minimized on the one hand to avoid surface damage and thus to increase the fiber lifetime and on the other hand to achieve the necessary spectral broadening. To our knowledge the fiber surface damage has not been discussed in the literature so far, even though it is a limiting factor in a real experiment dealing with sub-20 fs pulses of nJ energy. At this energy level the damage problem has been described for bulk transparent materials [8]. The lifetime of the fiber can be as short as some hours under the conditions above. Then a crater appears which leads to a lower transmission, worse beam quality, and a narrower SC. These limitations mean that the pulse energy has to be kept as low as possible for a given fiber and focusing conditions. Although longer pulses (50–100 fs) provide broader

SC in long PCFs [3, 7] and avoid the fiber damage, they have lower intensity at the entrance surface of the fiber, which has to be compensated by the fiber length to achieve prominent broadening. Moreover, in some experiments sub-20 fs pulses are needed. One example of such an experiment will be shown in Sect. 2.1 below.

In the paper we show and discuss two simple ways to increase the SC width at the same pulse energy and fiber length by (i) using a double-pulse technique and (ii) exploiting polarization effects. The first way is similar to that discussed earlier for two pulses of different colors [9] or different polarizations [10]. Our approach is much simpler because it includes additionally only one beam splitter of a certain thickness. The second way is to manipulate the polarization state of the input radiation, namely with the plane of the input electric field relative to the principal axes of the PCFs or the ellipticity of the pump [7, 11]. There are no theoretical publications to our knowledge on this subject, mainly because of difficulties in modeling azimuthal fiber asymmetry. This effect is certainly important in birefringent PCFs (BF PCFs) because the polarization plane of the output depends on the orientation of the fiber principal axis and the polarization of the incident radiation.

The paper consists of an experimental part devoted to the double-pulse effect and to the polarization effects. It also contains some data on the fiber damage. The second, theoretical, part contains the relevant numerical simulations. It is shown that the spectral broadening for the double-pulse regime is provided by the fusion of the pulses due to their interaction enhanced by the Raman self-scattering with the subsequent fission of the soliton complex. In the single-pulse regime the contribution of polarization effects to the SC characteristics is analyzed. It is demonstrated that the interaction of the polarization modes causes energy transfer between them depending on polarization state and dispersion. The contributions of the polarization-mode beating and the Raman self-scattering are analyzed as well.

2 Experimental setup and results

2.1 Double pulses

The laser system consists of a 11-fs, 16 nJ Ti:Sa oscillator [12] providing a spectrum of 700 to 900 nm. A small

✉ Fax: +43-1/58-8013-8799, E-mail: apolonski@tuwien.ac.at

fraction (15%, i.e. about 2 nJ) of the energy was split off with a 20 μm pellicle made of nitrocellulose which was positioned at 45° to the beam. This beam was used for the phase-stabilization loop [12] which allows the oscillator to generate pulses with a constant carrier envelope phase shift. The loop contains a piece of cobweb PCF (from the University of Bath) to generate the SC and a nonlinear interferometer in the so-called f -to- $2f$ scheme. The scheme utilizes the beat signal between the fundamental component at 530 nm and the frequency-doubled radiation of the 1060 nm component. The main part of the energy, transmitted through the pellicle, was used for the nonlinear experiment (photoemission from a solid target) [5] and had to be maximized. In this part a short piece of conventional single-mode fiber (1.5 mm) was used to broaden the initial spectrum from the oscillator, and a special compressor to produce 4 fs pulses. With longer initial pulses or lower energy it was impossible to produce sufficient broadening and then to achieve short pulses. Even a slight pulse-energy improvement is important in this part of the layout because the generated photocurrent scales with the third or fourth power of the intensity. According to theory only short (≤ 6 fs) pulses can produce a phase-sensitive photoemission signal.

In the phase-stabilization loop, a laser beam of approximately 40 mW of average power was injected into an 8 cm cobweb PCF of 2.2 μm core by using a Thorlabs objective. A similar objective was used for collimating the output radiation. Both the dispersion of the oscillator's output coupler and the objective were pre-compensated by a chirped mirror compressor so that the pulses injected into the PCF were almost chirp-free [7]. Broadened radiation (transmission through the PCF is about 30%) was then detected with an optical spectrum analyzer (Ando AQ-6315A). A waveplate was mounted in front of the PCF to change the polarization state of light coupled into the fiber. The relevant spectrum is shown in Fig. 1 (black curve). Note that a specific shape of SC and its width depend very much on the input-beam ad-

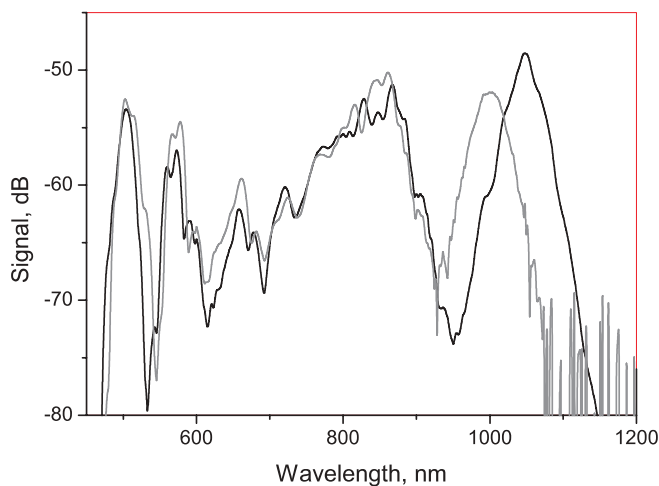


FIGURE 1 SC generated in a 8 cm cobweb PCF of 2.2 μm core with 11 fs pulses. *Gray curve*: a single pulse of 20 mW average power, *black curve*: double pulses separated at the entrance surface of the PCF by 150 fs of total power 40 mW

justment. In an attempt to maximize the power for the main nonlinear experiment, and considering that the two pulses reflected from the two surfaces of a pellicle are separated by almost 150 fs and do not overlap (and so would not be expected to interact) in the PCF, we then replaced the pellicle with a flat glass plate having a broadband antireflection coating on one side. Thus we increased the transmitted power for the nonlinear experiment. The power reflected from the plate became approximately two times less because of similar refractive indices of the original pellicle and the glass plate. The beam profiles in the two cases were similar. However, the detected spectrum was quite different; see Fig. 1 (gray curve). The clearly seen deficit in the IR part of the SC (up to 15%) can not be explained by the fiber adjustment or the pulse properties. The necessary SC width to provide reliable phase stabilization was then obtained by increasing the reflected part from the glass plate by 25% by changing the angle of the incident beam. Unfortunately, as a consequence of the higher pulse energy, fast damage of the PCF was then observed.

We did not use a thinner pellicle (giving a smaller time offset for the two pulses) to collect more data because such a beam splitter behaves like an oscillating membrane, decreasing the stability of the system which must be high to provide long-term phase stabilization. Nevertheless, we reproduced this experiment several times. The conclusion we made from this experiment is that, even though the pulses were initially separated by 150 fs, they interact in the 8 cm long PCF, thus providing additional spectral broadening.

2.2 Polarization effects

We have already shown that the polarization effects lead not only to the SC width variations, but also to its spectral shaping [7]. By exploiting these effects one can enhance a desirable part of the SC. Here we tried to check and modify the polarization states of the SC for different PCFs and different pumps with the aim of generating spectral wings of a desirable (the same) polarization plane and of the highest ellipticity.

In these experiments two Ti:Sa oscillators have been used. The first one with 11 fs pulses has already been described in Sect. 2.1. The second oscillator provided 6.5 fs pulses and had a spectrum spanning from 600 nm to almost 1000 nm (a description of the oscillator will be published elsewhere). For such a broad spectrum no waveplates exist and all polarization measurements were done by rotating the PCF's azimuth.

Two types of short pieces of PCFs were checked. One was a 6 mm long cobweb PCF with different core diameters of 1.6–3.0 μm from the University of Bath (both basic types used are shown in Fig. 2). The estimated birefringence of the fiber is 10^{-4} to 10^{-5} . Another birefringent (BF) PCF had been produced at OFS Laboratories (inset in Fig. 3). It had a 1.7 μm core diameter and the same length as the cobweb PCFs.

Focusing the radiation after the oscillators and compressors as well as collimation was done by using broadband objectives having flat dispersion in the range of 700–900 nm. As a result, the SC in the range of 440–1250 nm was generated in a 2.2 μm core diameter cobweb PCF (see Fig. 1). In the case of a BF PCF the SC generated covers the range of

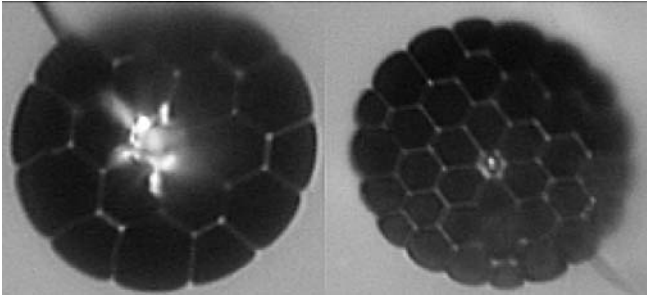


FIGURE 2 Damage spots in cobweb PCFs of two types

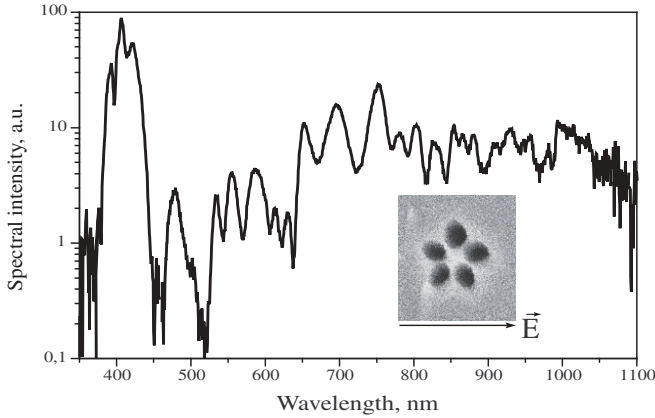


FIGURE 3 Generated SC in a 6 mm BF PCF of 1.7 μm core with 6.5 fs pulses. *Inset*: fiber structure and its orientation relative to the electric field of the incident pulse to provide coincidence of the incident and output pulse polarizations

380–1050 nm (Fig. 3). It contains a deep dip around 500 nm, which is rather typical for PCFs of this core diameter [7]. For example, for a 1.6 μm cobweb PCF the generated SC covers the range of 390–1040 nm with a deep dip from 500 to 650 nm. The throughput was up to 30% in the case of a 2.2 μm cobweb PCF and $\sim 10\%$ in the case of a BF PCF. We were interested in generating spectral wings with the same polarization state for experiments similar to that described in Sect. 2.1. For cobweb PCFs the wings generally have different polarization states and polarization planes depending on the azimuthal adjustment. In the case of a BF PCF the polarization plane depends only on the azimuthal fiber alignment and is the same for all spectral parts. The planes of the initial radiation and the output coincide if the former is aligned horizontally in the inset in Fig. 3. For cobweb PCFs it was nevertheless possible to adjust the planes for different (desirable) far-separated spectral components by rotating the fiber, whereas close spectral components (for example, 475 and 500 nm) can be of very different polarization states, almost in antiphase, and the rotation of the PCF is not sufficient.

The rotational symmetry for cobweb PCFs is 40° – 60° for 11 fs pulses and 180° for 6.5 fs pulses, but for the BF PCFs it is always 180° . The ellipticity of the output for the BF PCFs is 10–20 for the wings of the SC and ~ 5 for the central spectral part. For cobweb PCFs this value is less: for the wings it is 2–5 and for the central part it is 5–10 depending on the relative orientation of the polarization plane of the incident radiation and the web structure.

2.3 Fiber damage

As was mentioned in the Introduction, fiber damage is a serious problem for short-pulse applications. In some cases, PCFs degrade after some minutes of operation. Usually surface damage begins at the entrance facet of the fiber, then during long operation (some days) it appears at the exit facet. The beam structure at the fiber output in these cases contains a black ring which separates two parts of similar color. The outer part of the beam has quite different divergence than the inner part and normally can not be utilized. If damage is progressing, the inner part becomes smaller in area whereas the black ring becomes larger. Usually in PCFs the surface damage leads to a deficit in the IR part of the SC. In some cases the damage may freeze itself at the initial (or not advanced) stage and PCFs can efficiently operate over months even with a crater. The physics of the surface damage in fibers is not clear because of many factors which are not under full control: surface quality, external conditions (dust, humidity), and fiber mechanical properties. As for the last, BF PCFs have a slightly longer lifetime than that of cobweb PCFs. Contrary to a conventional fiber, where damage always means the appearance of a crater, in case of PCFs damage could lead to a nonsymmetric surface break (see Fig. 2), even in the shape of a scratch. This can be explained by the absence of perfect azimuthal mechanical symmetry.

3 Model and discussion

The study of the above-described phenomena is based on the scalar 1 + 1-dimensional numerical model. The nondissipative intra-fiber propagation of the initial sech-shaped chirp-free pulse (pulses) obeys the generalized nonlinear Schrödinger equation [13–17]. We distinguish two situations: (A) two pulses with coincident spectra co-propagate in the fiber without birefringence; (B) a single polarized pulse propagates in the birefringent fiber. The corresponding master equations have the following forms:

$$i \frac{\partial a}{\partial z} + \sum_{m \geq 2} \frac{i^m \beta_m}{m!} \frac{\partial^m a}{\partial t^m} = -\gamma (1 - f_R) |a|^2 a - \gamma f_R a \int_{-\infty}^t R(t') |a(z, t-t')|^2 dt', \quad (1A)$$

$$i \frac{\partial a_{1,2}}{\partial z} + i \delta_{1,2} \frac{\partial a_{1,2}}{\partial t} + \sum_{m \geq 2} \frac{i^m \beta_m^{(1,2)}}{m!} \frac{\partial^m a_{1,2}}{\partial t^m} = -\gamma \times (1 - f_R) \left\{ \left[|a_{1,2}|^2 + \frac{2|a_{2,1}|^2}{3} \right] a_{1,2} + \frac{a_{1,2}^* a_{2,1}^2}{3} \exp(\mp 2i\alpha z) \right\} - \gamma f_R \left\{ a_{1,2} \int_{-\infty}^t R(t') \left(|a_{1,2}|^2 + \frac{2|a_{2,1}|^2}{3} \right) dt' \right\} - \gamma f_R \times \left\{ \frac{a_{2,1}}{6} \int_{-\infty}^t R(t') (a_{1,2} a_{2,1}^* + a_{1,2}^* a_{2,1} \exp(2i\alpha z)) dt' \right\}. \quad (1B)$$

Here $a(z, t)$ is the slowly varying field amplitude (so that $|a|^2$ has a dimension of the intensity) [18], z is the propagation distance, t is the time measured in the reference frame moving with the pulse (polarization mode 1 in the case of coupled equations (1.B)), β_m is the m th-order dispersion coefficient, $\gamma = n_2\omega_0/c$ is the self-phase modulation (SPM) coefficient, f_R is the fraction of the stimulated Raman scattering (SRS) contribution to the nonlinear refractive index of the fiber, and $R(t)$ is the so-called Raman response function [19, 20]. Indices 1 and 2 in coupled equations (1.A) refer to the polarization modes, $\delta_2 = (n_2 - n_1)/c$ is the birefringence-induced group delay for the polarization mode 2 ($\delta_1 \equiv \emptyset$), and $\alpha = 2\pi(n_1 - n_2)/\lambda_0 = 2\pi/L_B$ (L_B is the polarization mode beat length).

It is convenient to normalize t to the initial pulse width t_p and z to the nonlinear length $L_{nl} = (\omega_0 n_2 I_0/c)^{-1}$ defined by the initial pulse intensity I_0 . The simulations were carried out on the mesh with the time step 1 fs (2^{13} points) and the spatial step $10^{-3} L_{nl}$.

3.1 Co-propagating double pulses

Let us consider the propagation of the initial pulse pair

$$a(t) = a_0 \left\{ \text{sech} \left[(t + \zeta)/t_p \right] + \text{sech} \left[(t - \zeta)/t_p \right] \exp(i\varphi) \right\}$$

(ζ is the half-interval between pulses and φ is their relative phase) in the absence of polarization effects (1.A). The parameters of the simulation, which approximately correspond to [2] and provide the best fit to the experiment, are $\varphi = 0$, $t_p = 6.25$ fs, $L_{nl} = 1$ cm, $N^2 = 5.7$, $L_d^{(2)}/L_d^{(3)} = 3$; $\lambda_0 = 800$ nm (maximum of the pulse spectrum) and lies in the anomalous-dispersion range ($N = \sqrt{L_d^{(2)}/L_{nl}}$ is the soliton number and $L_d^{(m)} = t_p^m/|\beta_m|$ is the m th-order dispersion length). For the sake of simplicity we neglect the dispersion terms with $m > 3$, although the higher-order dispersions affect the dynamics of the short pulses more strongly than that for the longer pulses.

Figure 4 presents the simulated spectra (averaged over the propagation length $L = 8$ cm corresponding to the experiment) without the SRS contribution ($f_R = 0$). It is obvious that the resulting spectrum for a single initial pulse (black solid curve) is narrower than that for a single initial pulse with doubled intensity (gray solid curve), because the latter allows the formation of three solitons as a result of the soliton-fission mechanism [21] whereas the former provides only two solitons. However, the essential growth of the input intensity aimed at the spectral broadening leads to the fast fiber damage (see above). An alternative method of spectral broadening is cross-phase modulation of two initially separated identical pulses (the nondegenerate cross-phase modulation of the spectrally separated pulses was considered in [22]). Although the maximum SPM can only be doubled (not tripled as in the nondegenerate case), this method is easier to realize experimentally.

The dashed curve in Fig. 4 shows the spectrum for the two initial pulses with $2\zeta = 100$ fs. It is seen that the spectrum is different by only an additional modulation due to the interference of the strongest solitons formed by the soliton-fission

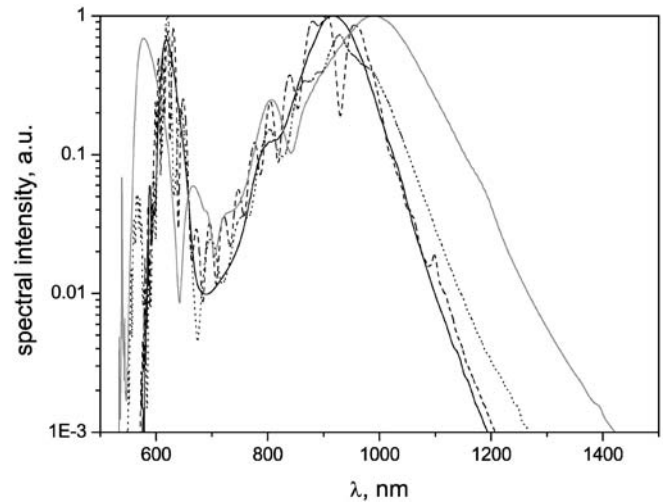


FIGURE 4 Spectra for $N^2 = 5.7$, $L_d^{(2)}/L_d^{(3)} = 3$, $T_{FWHM} = 2 \ln(1 + \sqrt{2})t_p = 11$ fs, $f_R = 0$, and $L_{nl} = 0.1$ cm. Single pulse (solid black), pulse with doubled intensity (solid gray), and double pulses separated by 100 fs (dashed) and 50 fs (dotted)

mechanism. The extra broadening is small. The analysis of the field evolution in the time domain demonstrates an attraction between the pulses, which is weak so that they collide at the distance $\approx 70L_{nl}$. Since the soliton formation is already finalized, the collision is almost elastic and there is no inter-pulse energy transfer providing spectral broadening. Nevertheless, even in this case the attracting force is stronger than that in the pure solitonic case (see [23]) and causes the collision at a relatively small distance. We assume that this phenomenon results from the modification of the pulse wings affected by the dispersive waves ($\beta_3 \neq 0$), which enforces the overlap of the pulse tails in analogy with the case considered in [24].

A decrease of the initial pulse interval enhances the overlap of the pulse tails and thereby the SPM-induced interaction (dotted curve in Fig. 4, $2\zeta = 50$ fs). The pulse collision then occurs at $z \approx 20L_{nl}$, when the soliton formation is not yet finalized. Their interaction has a pronounced nonelastic character (see Fig. 5) so that one pulse almost absorbs the other with the consequent extra spectral broadening (≈ 100 nm) due to the excitation of the additional dispersive and solitary waves (four in our case). The picture resembles that for the fission of the pulse with doubled intensity but in our case the peak intensity does not exceed I_0 along the full propagation length, which removes the danger of fiber damage.

Introduction of the SRS contribution ($f_R = 0.15$ [25]) into the simulation enhances the inter-pulse interaction significantly. As a result of the inertial contribution in the SPM through the phonon-mode excitation the range of the inter-pulse interaction widens. Hence the pulses collide at an early stage of propagation even for a 100 fs initial interval. The nonelastic character of this collision produces the extra spectral broadening (as was seen experimentally), which is larger than that in the absence of SRS (Fig. 6), and can reach 200 nm for $2\zeta = 50$ fs. Since nonelastic collisions for relatively large initial ζ are caused mainly by SRS, the red side of the spectrum is affected by this process to a greater extent than the blue side.

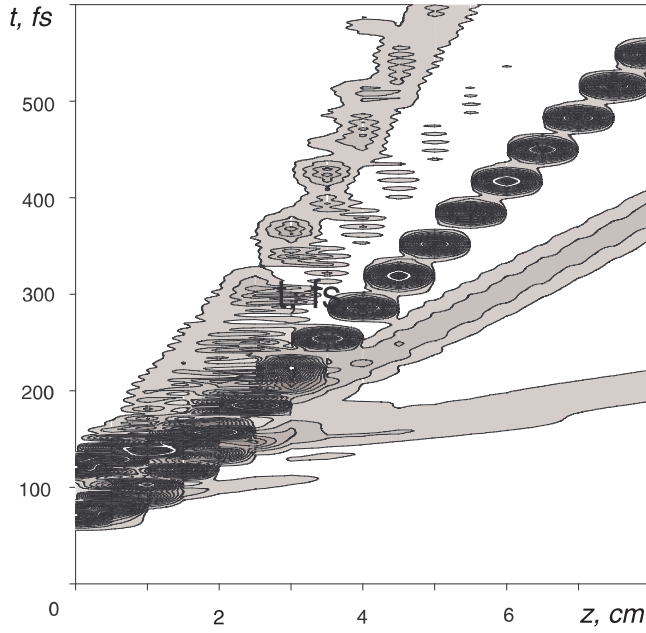


FIGURE 5 Contour plot of the field intensity (darker filling corresponds to the higher intensity level) for $2\zeta = 50$ fs. Collision takes place at a distance ≈ 1.5 cm from the fiber entrance facet. Other parameters correspond to Fig. 4

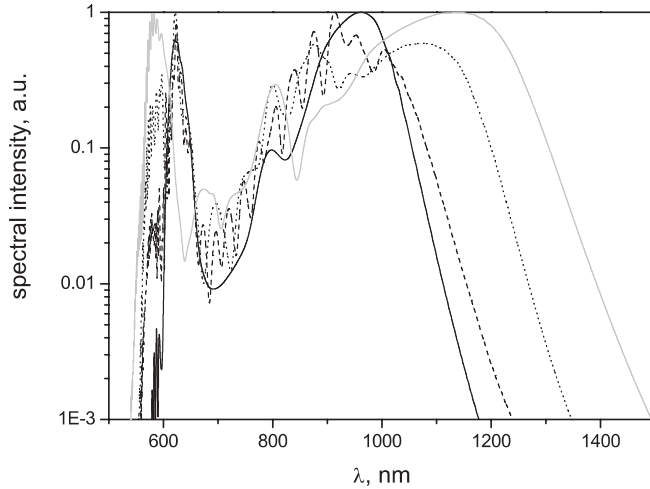


FIGURE 6 Spectra for $N_1^2 = 5.7$, $L_d^{(2)}/L_d^{(3)} = 3$, $T_{FWHM} = 11$ fs, $f_R = 0.15$, and $L_{nl} = 0.1$ cm. Single pulse (solid black), pulse with doubled intensity (solid gray), and double pulses separated by 100 fs (dashed) and 50 fs (dotted)

3.2 Polarization-mode interaction

An alternative way to control the spectrum without changing the incident pulse intensity or width can be realized by the use of the fiber birefringence. The dynamics of the propagation in this case is more complicated than the double pulses considered above due to presence of the phase-sensitive terms in (1.B).

At first let us consider the case of negligible SRS ($f_R = 0$). For small birefringence we can neglect the inter-mode beat. The corresponding condition in our case is $L_B > L = 8$ cm (L is the propagation length in the experiment), i.e. $|\Delta n| < 10^{-5}$. Then there is no visible dependence of the output spectrum on the polarization of the incident pulse if $\beta_m^{(1)} = \beta_m^{(2)}$. The

contribution of inter-mode beating for increasing Δn causes a redistribution of the spectral intensity between slow and fast axes: the slow polarization mode contributes to the blue side of the spectrum more strongly and vice versa the fast polarization mode is more intense on the red spectral side. However, the spectral width only changes slightly, although some additional modulation of the spectrum can appear.

When $|\Delta n| < 10^{-5}$ but $\beta_2^{(1)} \neq \beta_2^{(2)}$ ($f_R = 0$ and $\beta_3^{(1)} = \beta_3^{(2)}$), a pronounced dependence of the spectrum width on the polarization appears. In Fig. 7 solid (black and gray) curves show the spectra for the pure polarization modes (we suppose the simplest 90° polarization anisotropy). The second polarization mode (gray curve) has a smaller soliton number (weaker mode by convention) and thereby produces a narrower spectrum. A 45° orientation of the linear polarization of the incident pulse relative to the first polarization axis causes an energy transfer from the stronger mode (black dashed curve) into the weaker mode (gray dashed curve). The weaker mode increases on the blue side of the spectrum and the gap near 700 nm decreases. The transition to circular polarization reduces the spectral width (+ crosses in the figure) and there is a sensitivity of the spectrum (on its blue side) to the sign of the polarization rotation (\times crosses in the figure correspond to the opposite sign of the rotation).

The contribution of the beat for increasing $|\Delta n|$ decreases the spectral width, which becomes equal for both polarizations ($|\Delta n| \approx 10^{-3}$). Although the phase-sensitive term in (1.B) vanishes ($L_B < L_{nl}$) the interaction between modes does not disappear at the considered distance because this interaction decreases the relative group velocity (however, further propagation walks off the pulses one from the other). As before, the blue side of the spectrum is the more sensitive (especially in the weaker mode). We suppose that the stronger sensitivity of the blue spectral side to the polarization results from its dispersive nature: the intensity of the blue dispersive waves is defined by the energy transfer from the solitonic (red) part of the spectrum and is governed by their

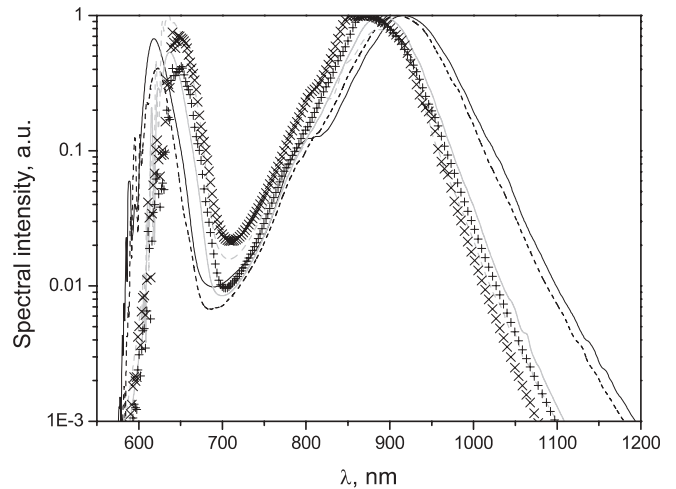


FIGURE 7 Spectra for $N_1^2 = 5.7$, $N_2^2 = 3.8$, and $L_d^{(2)}/L_d^{(3)} = 3$, other parameters correspond to Fig. 4. Pump pulse with the linear polarization at 0° (black solid curve), 45° (dashed curves, black – output at 0° , gray – output at 90°), and 90° (gray solid curve) relative to axis 1. + crosses correspond to the right circular polarization and \times crosses correspond to the left one

relative phase [26]. Hence, the phase-sensitive mechanisms (including polarization ones) can change this phase relation and thereby contribute to the dispersive-wave emission.

Addition of SRS causes some transformations in the above-described picture: (i) solitonic spectral spikes shift into the red side, (ii) the difference between strong and weak modes increases on the blue side of the spectrum, and (iii) the sensitivity of the spectral gap to the polarization state increases too.

4 Conclusion

Control of SC characteristics is of interest for numerous applications. Although shortening of the pump pulse decreases the soliton number and thereby reduces the spectral width of the SC, this allows making the propagation length shorter and diminishes the contribution of losses and spectral noise. The additional spectral broadening for short pulses with duration < 20 fs (up to the total one-octave width) can not be achieved by a simple increase of the pump intensity above a certain level because it inevitably leads to fiber damage. However, there are some alternative tools for the control of the SC characteristics: dynamical spectral widening due to double-pulse merging and using the fiber birefringence. We have analyzed these approaches both experimentally and theoretically. It was shown that the interaction of double pulses, which is enhanced by the Raman self-scattering, produces extra SC broadening (~ 100 nm) without any dangerous intensity growth. Also, we have analyzed the contribution of polarization effects to the SC characteristics. It was demonstrated that the nonlinear coupling of the polarization modes redistributes some energy between them and thereby adds a dependence of the spectral width on the polarization (linear as well as circular). This allows not only governing the spectral width but also controlling its structure, viz. changing the height of the dispersive (blue) spikes and the depth of the spectral dips.

ACKNOWLEDGEMENTS We are indebted to F. Krausz for his interest in this work. We thank T. Udem and R. Holzwarth for their help with a phase-stabilization loop. We appreciate the help of J. Dudley. This

work was supported by the Fonds zur Förderung der wissenschaftlichen Forschung (Project Nos. P15382 and M688) and partially by the Christian Doppler Gesellschaft. A. Apolonski dedicates this paper to the memory of his daughter.

REFERENCES

- 1 R. Alfano (Ed.): *The Supercontinuum Laser Source* (Springer, Berlin 1989)
- 2 J.C. Knight, J. Arriaga, T.A. Birks, A. Ortigosa-Blanch, W.J. Wadsworth, P.S.J. Russell: *IEEE Photon. Technol. Lett.* **12**, 807 (2000)
- 3 J.K. Ranka, R.S. Windeler, A.J. Stentz: *Opt. Lett.* **25**, 25 (2000)
- 4 A. Baltuška, Z. Wei, M.S. Pshenichnikov, D.A. Wiersma, R. Szipocs: *Appl. Phys. B* **65**, 175 (1997)
- 5 V.S. Yakovlev, P. Dombi, G. Tempea, C. Lemell, J. Burgdörfer, T. Udem, A. Apolonski: *Appl. Phys. B* **76**, 329 (2003)
- 6 S.T. Cundiff, J. Ye, H.L. Hall: *Rev. Sci. Instrum.* **72**, 3749 (2001)
- 7 A. Apolonski, B. Povazay, A. Unterhuber, W.J. Wadsworth, J.C. Knight, P.S.J. Russell, W. Drexler: *J. Opt. Soc. Am. B* **19**, 2165 (2002)
- 8 C.B. Schaffer, A. Brodeur, J.F. Garcia, E. Mazur: *Opt. Lett.* **26**, 93 (2001)
- 9 N. Karasawa, R. Morita, H. Shigekawa, M. Yamashita: *Opt. Commun.* **197**, 475 (2001); N. Karasawa, S. Nakamura, N. Nakagawa, R. Morita, H. Shigekawa, M. Yamashita: *IEEE J. Quantum Electron.* **QE-37**, 398 (2001)
- 10 N. Nishizawa, T. Goto: *Opt. Express* **10**, 256 (2002)
- 11 L. Tartara, I. Cristiani, V. Degiorgio, F. Carbone, D. Faccio, M. Romagnoli, W. Belardi: *Opt. Commun.* **215**, 191 (2003); F.G. Omenetto, A. Efimov, A. Taylor, J.C. Knight, W.J. Wadsworth, P.S.J. Russell: *Opt. Express* **11**, 61 (2003)
- 12 A. Apolonski, A. Poppe, G. Tempea, C. Spielmann, T. Udem, R. Holzwarth, T.W. Hänsch, F. Krausz: *Phys. Rev. Lett.* **85**, 740 (2000); A. Poppe, R. Holzwarth, A. Apolonski, G. Tempea, C. Spielmann, T.W. Hänsch, F. Krausz: *Appl. Phys. B* **72**, 373 (2001)
- 13 K.J. Blow, D. Wood: *IEEE J. Quantum Electron.* **QE-25**, 2665 (1989)
- 14 C.R. Menyuk: *IEEE J. Quantum Electron.* **QE-23**, 174 (1987)
- 15 C.R. Menyuk, M.N. Islam, J.P. Gordon: *Opt. Lett.* **16**, 566 (1991)
- 16 G.P. Agrawal: *Nonlinear Fiber Optics* (Academic, New York 2001) pp. 207, 304
- 17 J.M. Dudley, S. Coen: *Opt. Lett.* **27**, 1180 (2002)
- 18 T. Brabec, F. Krausz: *Phys. Rev. Lett.* **78**, 3282 (1997)
- 19 R.H. Stolen, J.P. Gordon, W.J. Tomlinson, H.A. Haus: *J. Opt. Soc. Am. B* **6**, 1159 (1989)
- 20 D. Hollenbeck, C. Cantrell: *J. Opt. Soc. Am. B* **19**, 2886 (2002)
- 21 A.V. Husakou, J. Herrmann: *Phys. Rev. Lett.* **87**, 203901 (2001)
- 22 L. Xu, N. Karasawa, S. Nakamura, R. Morita, H. Shigekawa, M. Yamashita: *Opt. Commun.* **162**, 256 (1999)
- 23 J.P. Gordon: *Opt. Lett.* **8**, 596 (1983)
- 24 B.A. Malomed: *Phys. Rev. A* **44**, 6954 (1991)
- 25 S. Smolorz, F. Wise, N.F. Borrelli: *Opt. Lett.* **24**, 1103 (1999)
- 26 A.V. Husakou, J. Herrmann: *J. Opt. Soc. Am. B* **19**, 2171 (2002)